



Parametric Investigation of Wavy Rectangular Winglets for Heat Transfer Enhancement in a Fin-and-Tube Heat Transfer Surface

S. K. Sarangi, D. P. Mishra[†] and P. Mishra

Department of Mechanical Engineering, Birla Institute of Technology, Mesra, Ranchi, India

[†]*Corresponding Author Email: diptimishraster@gmail.com*

(Received May 20, 2019; accepted August 13, 2019)

ABSTRACT

In this paper numerical simulations were performed utilizing Computational fluid dynamics code Fluent to investigate the thermo-fluid performance of a wavy rectangular winglet supported fin-and-tube heat exchanger with five inline rows of circular tubes. The influence of wave height, number of waves, wavy winglet length and winglet attack angle on the thermo-fluid performance of the fin-and-tube heat transfer surface has been examined under laminar flow conditions. Further the Plain and wavy rectangular winglets are placed together over different tube locations and their effect on heat transfer and flow resistance is also examined. An enhancement factor has also been discussed to summarize the overall thermo-fluid performance. The results show that increase in the wave height increase both heat transfer and pressure drop, and an optimum wave height could be decided based on the enhancement factor. It is also found that the increase in wavy winglet length guides the flow more effectively towards the tubes wake region. It is also observed that with increase in number of waves the heat transfer performance initially increases and then decreases as the wave pitch becomes very small. For wavy winglet supported heat exchanger the optimum attack angle is found out for maximum enhancement factor.

Keywords: Wavy rectangular winglet; Thermo-fluid performance; Enhancement factor; Number of waves; Fin-and-tube heat exchanger; Wave height.

NOMENCLATURE

A	cross-sectional area	Q	rate of heat transfer
A_{min}	minimum free flow area	Re	Reynolds number
A_T	total heat transfer surface area	T	temperature
B	span length	\bar{T}	total average temperature
C	specific heat of Aluminum	u	velocity in x-direction
CFD	Computational Fluid Dynamics	u_{in}	inlet velocity
C_P	specific heat of air	u_i, u_k	velocity component in i and k direction
D	tube diameter	VG	vortex Generator
D_h	hydraulic diameter	W_h	wave height
f	friction factor		
h	heat transfer coefficient	α	Thermal diffusivity
H	fin pitch	β	winglet attack angle
J_{abs}	absolute vorticity flux	ρ	density
k_a	thermal conductivity	μ	dynamic viscosity
L	flow length	η	enhancement factor
l	length of winglet	ω	vorticity
\dot{m}	mass flow rate		
n	Wave number	Subscripts	
Nu	Nusselt Number	al	aluminum
P	pressure	a	air
P_a	atmospheric pressure	b	baseline model
ΔP	pressure drop	$down$	domain bottom surface

in inlet parameter
o outlet parameter
up domain top surface
w wall

Superscripts

N normal to the cross-section

1. INTRODUCTION

Fin-and-tube heat exchanger finds extensive applications in many industrial applications such as refrigeration and air conditioning systems, for petrochemical cooling in chemical industries and for cooling of electronic equipment. Due to the limitation of space and size in many engineering applications the demand for compactness in these heat exchangers are increasing day by day. However, the air side convective resistance in these heat exchangers is generally very high owing to its thermo-physical properties. Different methods for enhancement of heat transfer includes active, passive and compound methods. Vortex generation using flow drivers such as wing and winglet is a passive heat transfer augmentation technique where the only external power required is for pumping of the fluid to overcome the pressure drop. These winglets form vortices close to the wake region of the flow field which facilitates better thermal mixing by modifying the boundary layer.

Edward and Alker (1974) compared the heat transfer performance produced by co-rotating and counter-rotating vortices and found the later one to be more effective. They reported for enhancement in heat transfer cube shaped VGs to be more efficient than delta shaped VGs. Russell *et al.* (1982) investigated the impact of various types of

VGs for heat exchanger having staggered rows of winglets and found best heat transfer results with the rectangular winglets. The performance of a delta winglet pair and single delta wing was experimentally studied by Fiebig *et al.* (1986) using liquid crystal thermography method. The delta wing type VG was found to deliver best local heat transfer enhancement. They conducted further experiments and found that counter-rotating vortices generated from a pair of rectangular and triangular type VGs improved the thermal performance. For unit vortex generator's area, triangular type VGs was found to be more effective than the rectangular one (Fiebig *et al.*, 1991). Tiggelbeck *et al.* (1994) found that at higher angle of attack and Reynolds number delta winglet pair had shown superior performance compared to rectangular a rectangular winglet pair. They also compared wing and winglet type VGs and reported higher heat transfer in case of winglet. Jacobi and Shah (1995) presented an excellent assessment of the heat transfer enhancement methods. Wang and Chang (1996) analyzed the thermo-fluid performance by varying tube rows, fin thickness and fin pitch. They found that the fin thickness does not affect the thermo-fluid performance. They also reported that the variation in tube row number and fin pitch have negligible effect on friction factor

and heat transfer coefficient respectively. Chen *et al.* (1998a, 1998b) examined the thermo-fluid performance with delta winglet supported finned oval tube. They investigated the winglet attack angle, aspect ratio and location of the winglet pairs. They also compared the finned oval tube with 1-3 rows of winglets. Sohankar and Davidson (2001) numerically examined the block shaped VGs in a three-dimensional channel. They found that the thicker blocks generated stronger and longer longitudinal vortices which enhance the thermal mixing. Further, they suggested that for studying the transitional flow QUICK scheme should not be used due to its dissipative nature. Gentry and Jacobi (2002) considered developing channel flow and flat plate flow supported with a delta wing for vortex generation to analyze the thermo-fluid performance. They also provided a measure of the vortex strength using vane-type vortex meter. Leu *et al.* (2004) conducted experiments in inclined block shaped VG supported plate-fin-and-tube heat exchanger using a water tunnel and infrared thermo vision system respectively, for visualization of flow structure and temperature distribution. They found that about 25% of the total fin area can be reduced if the winglet supported geometry is used instead of the Plain fin geometry. Pesteei *et al.* (2005) presented optimum stream-wise and span-wise winglet location for maximum enhancement in heat transfer. Joardar and Jacobi (2007, 2008) reported that the "common-flow-up" placement of winglet compresses the thermally isolated region behind the tube, delays the flow separation and also modifies the temperature field at the adjacent tube's surface by causing flow impingement.

Chu *et al.* (2009) examined numerically the upstream and downstream placement of VGs in staggered tube type fin-and-oval-tube heat exchanger and found more effective heat transfer enhancement for placement of VGs in the downstream of tubes. Lemouedda *et al.* (2010) used CFD, Genetic algorithm and response surface methodology together for optimizing the winglet attack angle. Optimal sets of attack angle were presented for Re varying from 200-1200. Wu and Tao (2011) investigated the effect of variable tube diameter of two tube row fin-tube surface on the heat transfer. They found enhanced thermo-fluid performance on using smaller diameter tubes in the first row.

The thermo-fluid performance of a fin-and-tube heat exchanger was examined numerically with inline and staggered array of winglets by He *et al.* (2013). They found that an attack angle of 10° provided greater thermo-fluid performance. They also concluded that the thermo-fluid performance is better in staggered array case compared to inline one. Li *et al.* (2014) studied the heat transfer

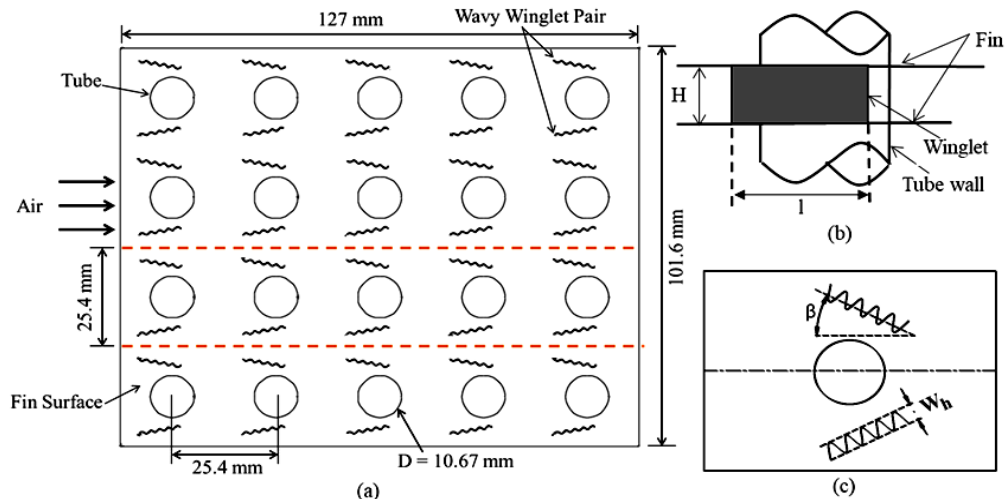


Fig. 1. (a) Schematic top view of a fin-and-tube heat exchanger showing wavy rectangular winglets, (b) Exaggerated side view around the tube showing the winglet height (H) and (c) Exaggerated top view around the tube showing the attack angle (β) and wave height (W_h).

performance by varying fin pitch and winglet length of a fin-and-tube heat exchanger for radiantly arranged delta winglets over different tubes with staggered arrangement. Wang *et al.* (2015a) performed experiments and compared the performance of plain fin model and semi dimple VGs for different fin pitch and tube row number. They conducted further experiments to compare the semi dimple configuration with louver and plain fin configuration (Wang *et al.*, 2015b). The semi dimple VGs outperforms the other considered models for frontal velocities lower than 2 m/s. Sinha *et al.* (2016) investigated the inline and staggered arrangement of winglets and tubes. In recent years, few studies have been presented on optimum winglet location. Arora *et al.* (2015) and Sarangi and Mishra (2017) respectively used the delta and Rectangular winglet pairs in “common-flow-up” arrangement with inline tube orientation in a fin-and-tube heat exchanger to investigate the optimum winglet locations. Sarangi *et al.* (2019) extended their research to five inline tubes supported with plain rectangular winglets and found out optimum winglet locations for highest enhancement factor. Similar investigations were performed by Naik and Tiwary (2018) with “common flow down” winglet orientation.

Chimres *et al.* (2018) reported that elliptical winglet with 45° attack angle and 130° trailing edge angle to delivered best heat transfer performance. Lu and Zhai (2019) numerically examined the effect of change in VG curvature and attack angle on the thermo-fluid performance of the heat exchanger. Wang *et al.* (2019) considered streamlined tube configuration to augment the overall thermo-fluid performance. They explained the formation of wake region using Kamran vortex street theory. Ke *et al.* (2019) used CFD simulations and optimization techniques to optimize the VG attack angle both for wavy and plain fin type finned-tube heat exchanger. Kobayashi *et al.* (2019) used topology optimization

method to design effective winglet configurations in two staggered row fin-and-tube heat exchanger.

The existing literature confirms the enormous potential of VGs as a heat transfer enhancement tool. The effect of wavy winglet pairs as heat transfer augmentation tool has not been studied previously and this has motivated the authors for present study. This paper numerically investigates the optimum number of waves, wave height, wavy winglet length, optimum location of combined Plain and wavy rectangular winglet pair, and optimum attack angle for winglet pairs with a “common-flow-up” orientation.

The Nusselt number and friction factor are used for the assessment of the performance of heat transfer and pressure drop respectively whereas the overall thermo-fluid performance has been estimated using enhancement factor for present heat exchanger model. The authors believe that the modified winglet configuration will be helpful in designing compact heat exchange devices.

2. MATHEMATICAL FORMULATION

2.1 Physical and Computational Model

Figure 1(a) shows the top view of a typical fin-and-tube heat exchanger with inline arrangement of tubes. The wavy rectangular winglet pair with height equal to fin spacing (3.63 mm) and length same as tube diameter (10.67 mm) is placed symmetrically over the tube as shown in Fig. 1(b) and Fig. 1(c). The flow domain with flow length 127 mm, span length 101.6 mm and fin pitch 3.63 mm (Joardar and Jacobi, 2007) is supported with “common-flow-up” orientated winglet pairs.

The region shown within the dashed lines in Figs. 2(a) and 2(b) is selected as the computational domain due to the symmetric orientation. Both, the longitudinal and transverse tube pitch are

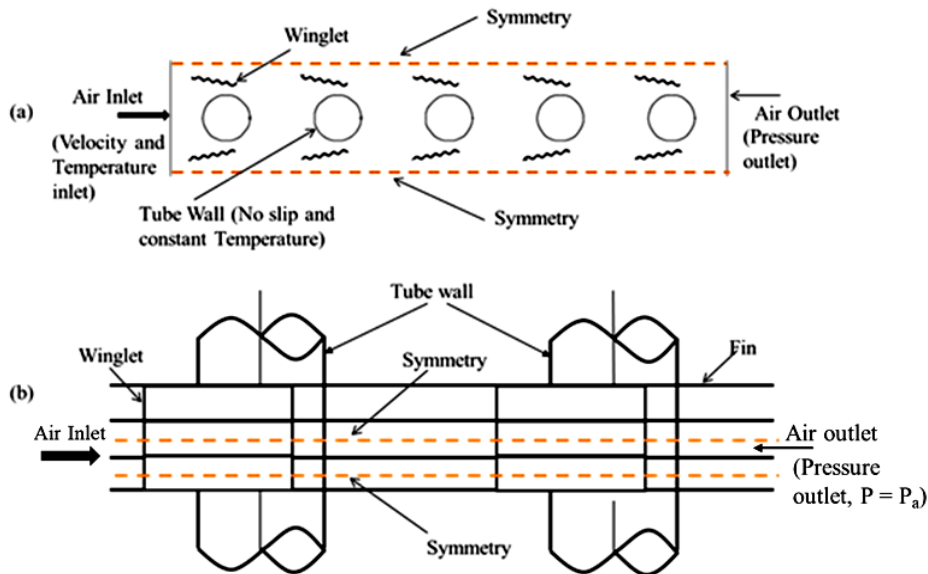


Fig. 2. (a) Top view, and (b) side view (shown for two tubes only) of the computational domain with applied boundary conditions.

considered to be 25.4 mm. The inlet air temperature is maintained at 310.6 K. The temperature of tube wall is set constant at 291.77 K owing to the high heat transfer coefficient fluid flowing inside the tube and conductivity of the wall of wall material (Aluminum).

2.2 Governing Equations

Following equations are required to be solved for the laminar, incompressible and steady flow:

The mass and momentum conservation equation are solved to compute the velocity field.

$$\text{Continuity equation: } \frac{\partial}{\partial x_i} (\rho u_i) = 0 \quad (1)$$

Momentum equation:

$$\frac{D}{Dt} (\rho u_i) = \frac{\partial}{\partial x_i} \left(\mu \frac{\partial u_k}{\partial x_i} \right) - \frac{\partial p}{\partial x_i} \quad (2)$$

Energy equation is solved to compute the temperature field.

$$\text{Energy equation: } \frac{D}{Dt} (\rho T) = \frac{\partial}{\partial x_i} \left(\frac{k_a}{C_p} \frac{\partial T}{\partial x_i} \right) \quad (3)$$

The conduction equation is solved to compute the temperature field in the fin and VGs.

$$\text{Conduction equation: } \frac{\partial^2 T}{\partial x_i^2} = \frac{1}{\alpha} \frac{\partial T}{\partial t} \quad (4)$$

$$\text{Where } \alpha = \frac{k_{al}}{(\rho_{al} C)}$$

The variation of air density with temperature follows the ideal gas equation.

For the operating temperature range (291.77 K-310.6 K) the thermal conductivity k and the dynamic viscosity μ are assumed to be constant.

2.3 Boundary Conditions

The computational domain is imposed with the following boundary conditions as shown in Fig. 2:

Domain inlet:

Uniform velocity u_{in} and temperature T_{in} at the inlet boundary

Zero velocity along y and z -direction.

$$v = w = 0.$$

The boundary conditions for upper and lower boundaries are set as symmetric. :

$$\frac{\partial u}{\partial z} = \frac{\partial v}{\partial z} = 0, w = 0, \frac{\partial T}{\partial z} = 0$$

The side boundaries are imposed with Symmetric boundary conditions.

$$\frac{\partial u}{\partial y} = \frac{\partial w}{\partial y} = 0, v = 0, \frac{\partial T}{\partial y} = 0$$

Domain outlet: The upper and lower boundaries are given Symmetric boundary conditions:

$$\frac{\partial u}{\partial z} = \frac{\partial v}{\partial z} = 0, w = 0, \frac{\partial T}{\partial z} = 0$$

The side boundaries are imposed with Symmetric boundary conditions:

$$\frac{\partial u}{\partial y} = \frac{\partial w}{\partial y} = 0, v = 0, \frac{\partial T}{\partial y} = 0$$

The domain outlet is imposed with pressure outlet boundary condition. As the fluid leaves the heat

exchanger outlet it is exposed to the surrounding atmospheric pressure i.e. $p = p_a$. For the simulation we have set zero gauge pressure.

Fin surface: Coupled and no-slip condition at the lower and upper boundaries.

Tube surface: Isothermal boundary condition and No-slip condition.

2.4 Computation of Heat Transfer and Fluid Flow Parameters

To assess the heat exchanger performance, following parameters have been computed (Joardar and Jacobi, 2007):

$$\text{Overall heat transfer, } Q = m c_p (\bar{T}_o - \bar{T}_{in}) \quad (5)$$

Where,

$$\bar{T} = \frac{\iint_A \rho u T dA}{\iint_A \rho u dA}$$

$$\text{LMTD, } \Delta T = \frac{(T_w - \bar{T}_{in}) - (T_w - \bar{T}_o)}{\ln[(T_w - \bar{T}_{in}) / (T_w - \bar{T}_o)]} \quad (6)$$

$$\text{Hydraulic diameter, } D_h = 4 \left(\frac{A_{\min} \cdot L}{A_T} \right) \quad (7)$$

$$\text{Reynolds number, } Re = \frac{\rho u_{in} D_h}{\mu} \quad (8)$$

$$\text{Nusselt number, } Nu = \frac{h D_h}{k_a} \quad (9)$$

$$\text{Heat transfer coefficient, } h = \frac{Q}{A_T \cdot \Delta T} \quad (10)$$

$$\text{Friction factor, } f = \frac{\Delta p}{\frac{\rho u_{in}^2}{2} \frac{A_T}{A_{\min}}} \quad (11)$$

Enhancement factor as defined by Caliskan (2014) and Sarangi *et al.* (2019):

$$\eta = \left(\frac{Nu}{Nu_b} \right) \left(\frac{f}{f_b} \right)^{-1/3} \quad (12)$$

Absolute vorticity flux,

$$J_{abs}^N = \frac{1}{A(x)} \iint_{A(x)} |\omega^N| \times dA \quad (13)$$

2.5 Numerical Methods

Computational fluid dynamics tool Fluent-17 has been used for discretizing the governing equations with proper boundary conditions. Hexahedral meshes are used to mesh the entire computational domain as shown in Fig. 3. The convective terms shown in the governing equations have been solved initially using first order upwind scheme. Then by

using second-order upwind scheme the results improved marginally (about 0.6%). Pressure and velocity field are coupled using SIMPLE algorithm. The solutions were said to be converged for continuity and momentum when their residuals falls below 10^{-3} and that for energy falls below 10^{-6} .

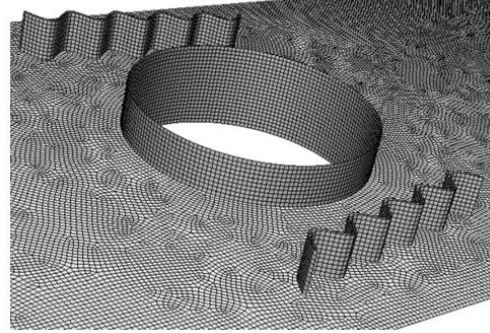


Fig. 3. Mesh system around the wavy rectangular winglet and tube.

3. RESULTS AND DISCUSSION

3.1 Grid independence and Validation of Numerical Results

To ensure a balance between the computational accuracy and size, the computational domain shown in Figs. 2(a-b) with structured meshing is refined until the flow field solutions were found to be grid independent. The grid test is performed for the baseline model with $Re = 650$.

Initially a coarse mesh (7,24,564) is selected and the mesh is subsequently refined to 19,27,784. However, Table 1 shows that the variation in Nu beyond grid size 17,89,494 is below 0.5%. Thus, the cell size corresponding to mesh number 17,89,494 has been selected to perform the simulations for the present investigation. Similar optimum grid refinement test is conducted for the wavy and plain rectangular winglet supported models.

Table 1 Variation of Nu with mesh size

Mesh size	Nu
7,24,564	3.95
10,13,264	4.37
13,54,184	4.72
15,48,366	4.79
17,89,494	4.81
19,27,784	4.83

In Fig. 4 the present CFD results have been compared against the available experimental results of Joardar and Jacobi (2008) for the baseline case. The plot of heat transfer coefficient and pressure drop shows that the obtained CFD results are in good agreement with the experimental results of Joardar and Jacobi (2008) with 10% of maximum

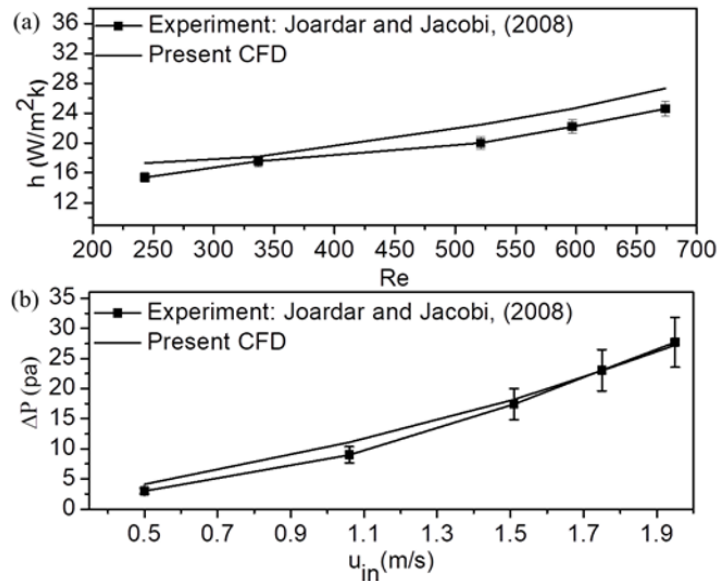


Fig. 4. Validation of numerical results for baseline case: (a) Heat transfer coefficient as a function of Reynolds number, and (b) pressure drop as a function of frontal velocity.

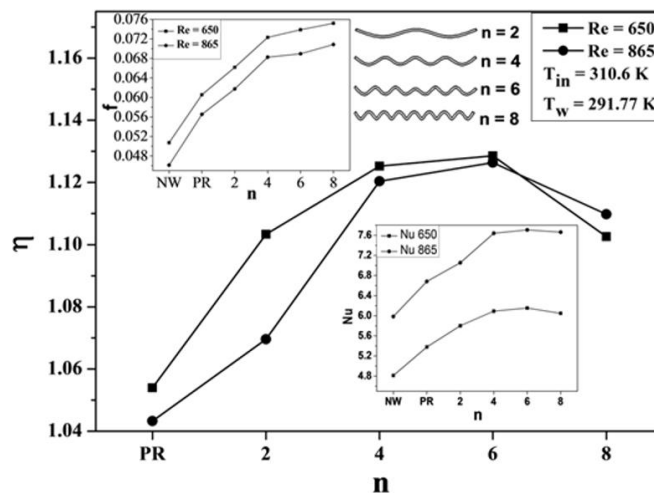


Fig. 5. Effect of wave number on heat transfer and flow parameters.

deviation. The uncertainty in the measurements of heat transfer coefficient and pressure drop were reported $\pm 4\%$ and $\pm 15\%$ respectively by Joardar and Jacobi (2008).

The current CFD results have a good agreement with the experiment results indicate appropriate numerical model has been selected to predict the fluid flow and heat transfer characteristics of heat exchanger.

3.2 Effect of Number of Waves on Thermo-Fluid Performance

In this section effect of increase in number of waves (2, 4, 6, and 8) of the wavy rectangular winglet pair with fixed wave height and winglet length has been discussed. The winglet pairs are placed at an attack angle of 10° (He *et al.*, 2013) with a fixed stream-wise and span-wise winglet position.

The Nusselt number plot in Fig. 5 shows Nu is enhanced up to wave number $n = 6$. The winglet's "common-flow-up" arrangement forms a converging section with the tube surface. The fluid gets accelerated on passing through this constricted zone and impinges on the adjacent tube surface resulting modification of boundary layer and improvement of local heat transfer. The velocity magnitude contours with different winglet geometries are shown in Figs. 6(a-b). The thermally isolated region behind the winglet supported tube is relatively larger in case of Plain rectangular winglet (Fig. 6(a)) compared to the wavy rectangular winglet supported model (Fig. 6(b)). Also due to the wavy nature of the winglet surface the generated vortices results in swirling motion and are advected along the stream. These vortices cause enhanced mixing of the mainstream flow with the cold fluid in the wake zone. This results in modification of the thermal boundary layer and enhancement in the

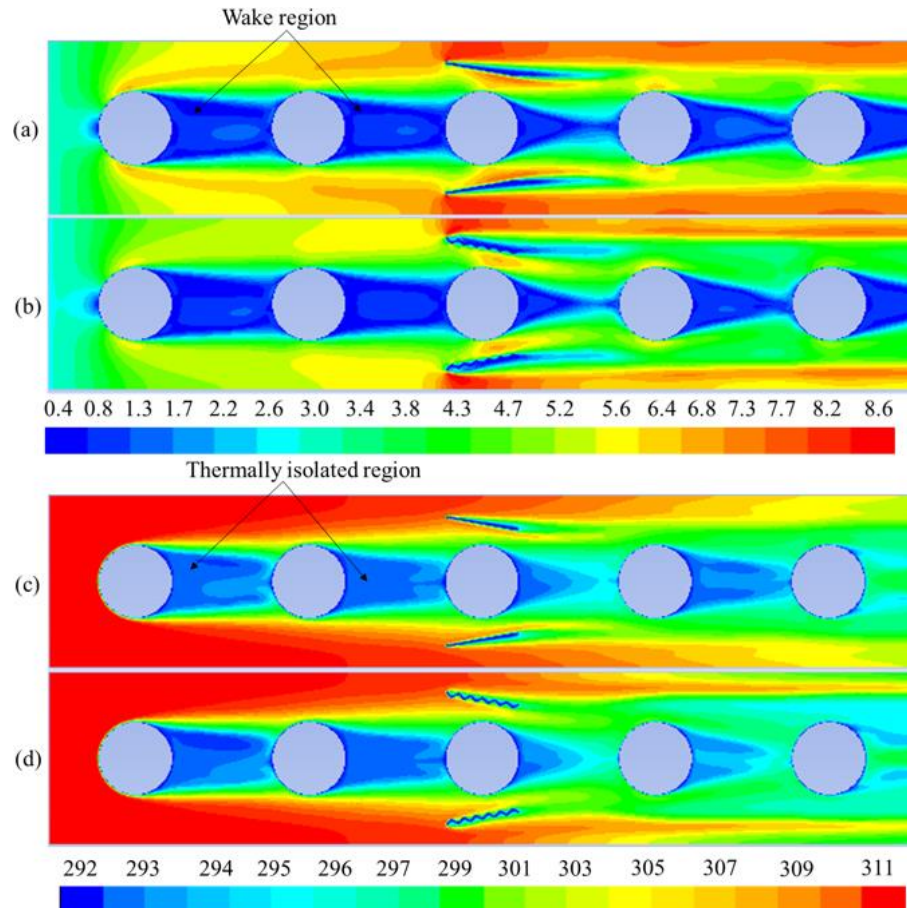


Fig. 6. Velocity contours (unit: m/s) and Temperature contours (unit: K) over the fin surface: (a) velocity contours for Plain rectangular winglet, (b) velocity contour for $n = 6$, (c) temperature contours for Plain rectangular winglet, and (d) temperature contours for $n = 6$.

local heat transfer at the wake region of the winglet supported tube. It can be clearly visualized from Figs. 6(c-d) the temperature within the wake region increases when the wavy rectangular winglet pair is employed (Fig. 6(d)) instead of Plain winglet pair.

This clearly indicates greater thermal mixing is realized for wavy rectangular winglet supported model (Fig. 6(d)) compared to the Plain rectangular winglet model (Fig. 6(c)). Thus, the combined effect of flow impingement and wavy nature of the winglet results in enhanced heat transfer. However, the wave pitch continuously decreases with increase in number of waves for a fixed winglet length. When the number of waves is increased beyond $n = 6$, the wave pitch becomes very small and the waviness of the winglet becomes ineffective for effective mixing of fluid within the wake zone. Thus, the enhancement in heat transfer is insignificant beyond $n = 6$.

Usually the enhancement in heat transfer is attained at the cost of some additional pressure drop. As the fluid moves between the crest and trough of the wavy rectangular winglets it suffers additional pressure drop and the friction factor continuously increases which can be seen in Fig. 5. An enhancement factor is also plotted in Fig. 5 to account for the overall performance of the heat

exchanger. The plot shows that the enhancement factor rises up to $n = 6$ and then it falls. Therefore, based on the obtained CFD results an optimum wave number of $n = 6$ could be decided for both the $Re = 650$ and 865 beyond which the pressure drop dominates the heat transfer enhancement. This results in fall of the enhancement factor for $n = 8$.

3.3 Effect of Wave Height on Thermo-Fluid Performance

In this section effect of variation in wave height of the wavy rectangular winglet pair with fixed wave pitch, wave number and winglet length has been discussed. The winglet pairs are oriented in "common-flow-up" arrangement at an attack angle of 10° .

The wave height of the wavy winglet is varied 0.3-1.2 mm with an interval of 0.15 mm. Figure 7 shows the absolute vorticity flux as a function of wave height. The secondary flow intensity continuously increases with the increase in wave height. These vortices form strong swirling motion at the immediate downstream of the winglets and results in greater transport of the cold fluid from tubes wake region to the mainstream passage.

It can be clearly visualized from Figs. 8(a-b) the wake zone of the winglet supported tube gets

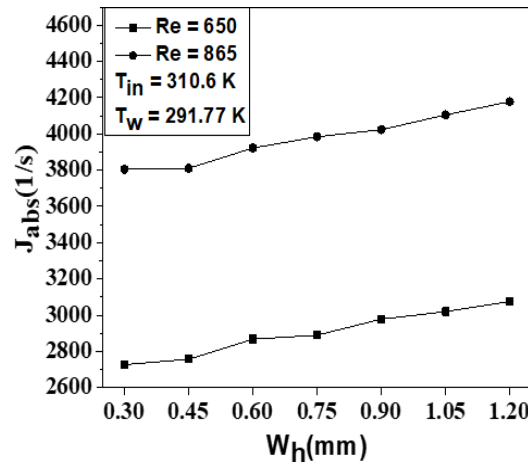


Fig. 7. Variation of Absolute Vorticity Flux with Wave Height.

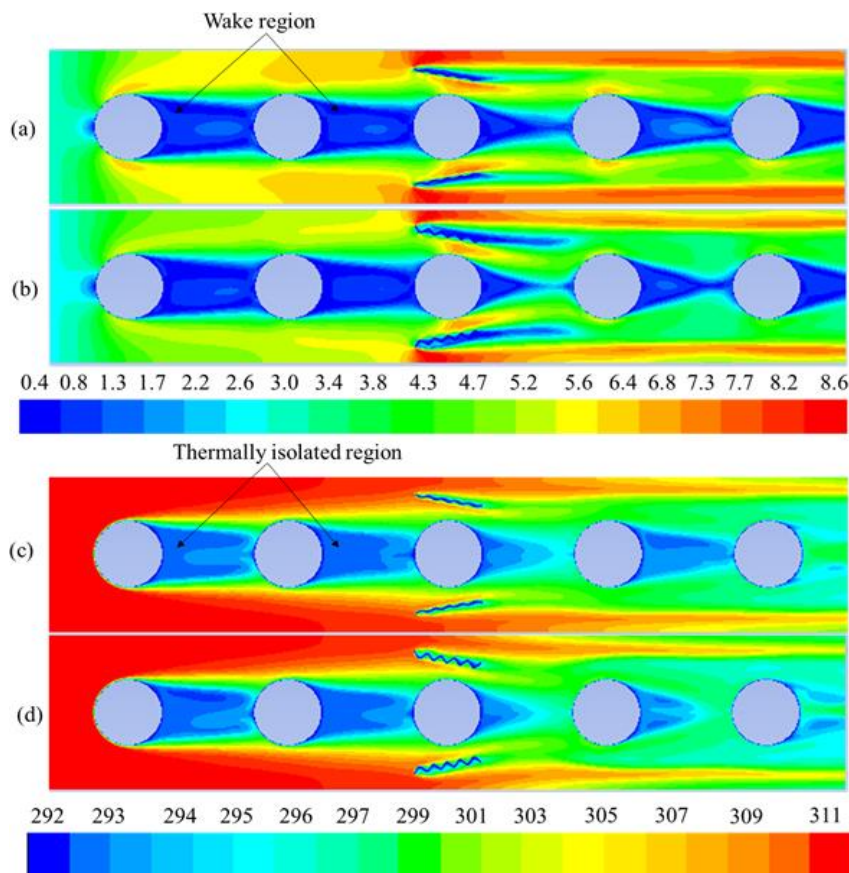


Fig. 8. Velocity contours (unit: m/s) and Temperature contours (unit: K) over the fin surface: (a) velocity contours for $W_h = 0.3$ mm, (b) velocity contours for $W_h = 0.9$ mm, (c) temperature contours for $W_h = 0.3$ mm, and (d) temperature contours for $W_h = 0.9$ mm.

compressed when the wave height is increased to 0.9 mm from 0.3 mm. It can also be visualized from Figs. 8(c-d) the temperature in wake zone of the winglet supported tube increases with the advancement in the wave height from 0.3 mm to 0.9 mm. This clearly indicates the higher wave height facilitates improved thermal mixing and enhanced local heat transfer performance which is consistent with the plot of Nusselt number in Fig. 9.

Variation in friction factor with wave height is also

plotted in Fig. 9. With the increase in wave height the winglet's span increases and offers greater resistance to the flow. As a result, for both $Re = 650$ and 865 , there is a sharp rise in the friction factor with advancement in wave height. The parameters Nu and f alone are insufficient to decide an optimum wave height and therefore an enhancement factor is also presented in Fig. 9. With the increase in the wave height from 0.3 mm to 0.9 mm the enhancement factor increases continuously

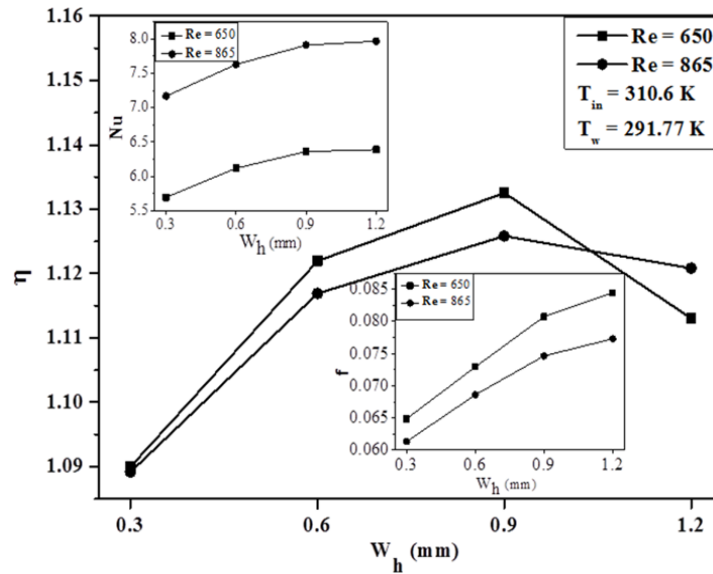


Fig. 9. Effect of wave height (W_h) on heat transfer and fluid flow parameters.

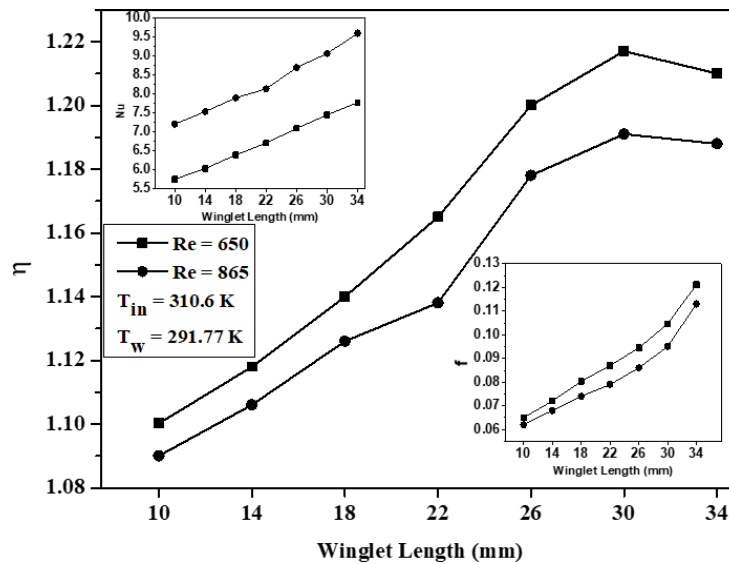


Fig. 10. Effect of winglet length (l) on heat transfer and fluid flow parameters.

and then drops. Thus, based on the present simulated results an optimum wave height of 0.9 mm could be decided beyond which enhancement in heat transfer is marginal whereas the pressure drop is considerably higher.

3.4 Effect of Winglet Length on Thermo-Fluid Performance

Effect of length of the wavy rectangular winglet on the thermo-fluid performance has been investigated with constant wave height and wave pitch. The winglets with “common-flow-up” orientation are kept at an attack angle of 10° . The winglet length is varied from 10 mm to 34 mm with an interval of 4 mm.

Figure 10 shows the variation in Nusselt number with length of the wavy rectangular winglet pair.

The plot shows that with advancement in the wavy winglet length the Nusselt number rises continuously. Figures 11(a-b) shows with the increase in the winglet length the flow is more effectively guided towards the tubes wake region. As a result, thermally isolated region is compressed significantly. Also, with increasing winglet length the frontal area increases, and larger volume of flow is guided towards the wake region of wavy winglet supported tube. The narrow converging region formed between the winglet and the tube accelerates the incoming flow which then impinges on the front section of the adjacent tube. This causes modification of the thermal boundary layer and results in local enhancement in heat transfer. Also, Figs. 11(c-d) shows that the temperature within the wake zone rises when the winglet length is increased.

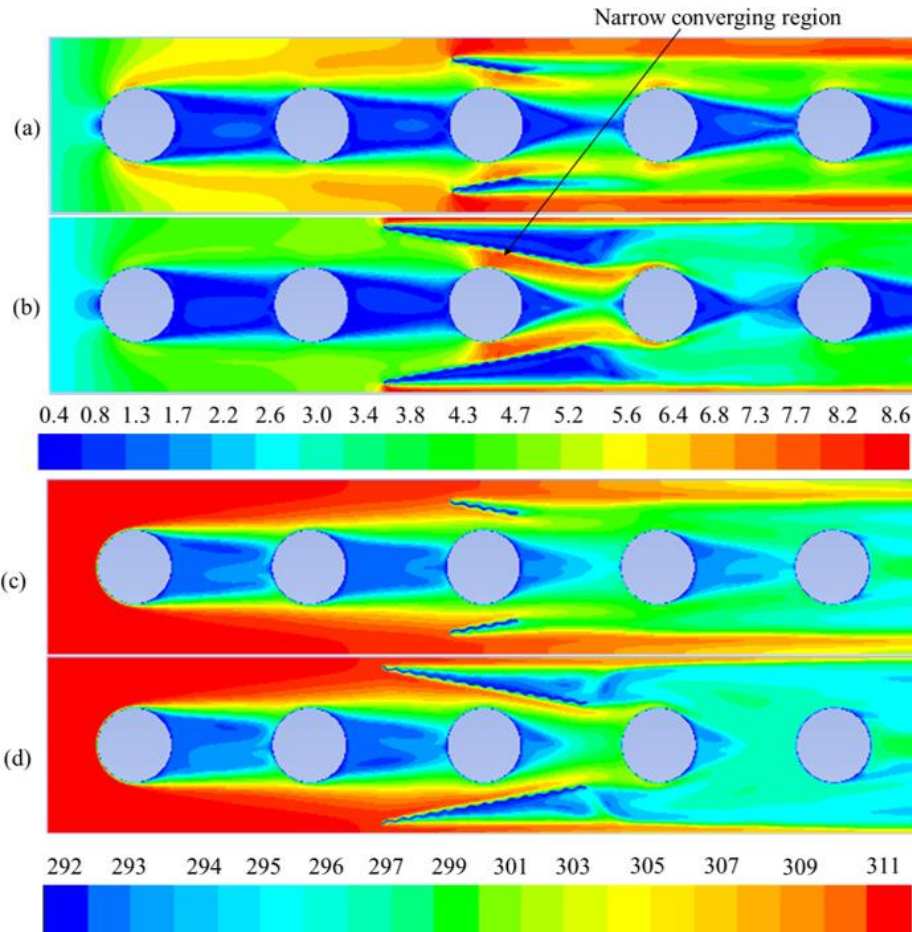


Fig. 11. Velocity contours (unit: m/s) and temperature contours (unit: K) over the fin surface for different winglet length: (a) velocity contours for $l = 10$ mm, (b) velocity contours for $l = 30$ mm, (c) temperature contours for $l = 10$ mm, and (d) temperature contours for $l = 30$ mm.

This clearly indicates with the increase in winglet length greater thermal mixing is achieved between the mainstream flow and the cold fluid in the wake region. However, with the increase in winglet length the form drag of the winglet pairs increases due to the increase in its frontal area. As a consequence, the friction factor rises rapidly as shown in Fig. 10.

To summarize the overall influence of the increase in the winglet length an enhancement factor is also plotted in Fig. 10. The plot shows that the enhancement factor rises continuously with the advancement in the wavy winglet length, attains its highest value at 30 mm and then drops. Thus, based on the present numerical results an optimum winglet length of 30 mm could be decided beyond which the pressure drop dominates the heat transfer and the overall thermo-fluid performance deteriorates.

3.5 Effect of Combined Plain and Wavy Rectangular Winglet on Thermo-Fluid Performance

Effect of combination of Plain and wavy rectangular winglet pair is investigated by placing them separately over different tubes. Fifth tube is

not supported by either the wavy or plain rectangular winglets as this winglet location does not cause flow impingement due to the unavailability of any further tube downstream. The placement of winglet thus can be written as $PiWj$ where, i and j ranges 1-4, for $i \neq j$. The winglets are placed with an attack angle of 10° .

Table 2 shows the variation in the performance parameters against various combinations of placement of a plain and a wavy rectangular winglet pair. Table 2 shows that a higher value of Nusselt number is obtained whenever the VGs are positioned near the first three tubes. The flow velocity near to the inlet is higher and it reduces as the flow advances downstream. The winglet when placed over the first three tubes forms a converging section with the tubes and accelerates the incoming flow. This high velocity fluid then impinges at the front section of the adjacent tube causing modification in boundary layer and improvement in local heat transfer performance. However, when either of the Plain or wavy rectangular winglet pair is kept near the fourth tube the flow velocity approaching the winglets reduces after it interacts with the first three tubes. As a result, the flow impingement is not effective enough to cause

Table 2 Variation of thermo-fluid performance parameters as a function of placement of combined Plain and wavy rectangular winglet pairs over different tubes

Winglet combination	Re = 650			Re = 865		
	Nu	f	η	Nu	f	η
NW	4.81	0.05071	1	5.98	0.046118	1
P1W2	6.75	0.08973	1.160	8.49	0.084118	1.161
P1W3	6.69	0.08904	1.153	8.22	0.082005	1.134
P1W4	6.53	0.08462	1.146	8.15	0.080286	1.132
P2W1	6.74	0.09157	1.150	8.44	0.086267	1.144
P2W3	6.93	0.08295	1.222	8.54	0.076651	1.204
P2W4	6.50	0.07844	1.168	8.03	0.074189	1.146
P3W1	6.80	0.08965	1.169	8.34	0.084083	1.141
P3W2	6.69	0.08613	1.166	7.88	0.077626	1.108
P3W4	6.52	0.07758	1.176	8.07	0.072586	1.159
P4W1	6.67	0.08732	1.157	8.26	0.083201	1.133
P4W2	6.57	0.08347	1.157	8.15	0.079043	1.138
P4W3	6.54	0.08283	1.154	7.72	0.077104	1.086

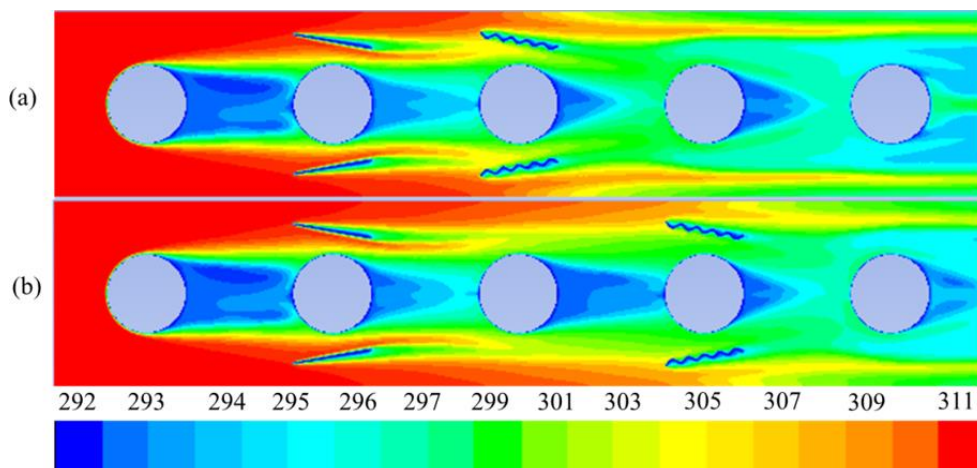


Fig. 12. Temperature contours over the fin surface for various combinations of Plain and wavy rectangular winglet: (a) Temperature contours for P2W3, and (b) Temperature contours for P2W4.

significant heat transfer enhancement. Figure 12(a) clearly shows that the temperature within the wake zone is higher when wavy winglet pair is employed near the third tube compared to its placement over the fourth tube (Fig. 12(b)). This clearly indicates placement of wavy winglet pair near the third tube facilitates greater thermal mixing in the wake region. Thus, placement of wavy or plain winglet pairs near the first three tubes is most advantageous for improved heat transfer performance. Table 2 also indicates that the friction factor is considerably higher for placement of either the Plain or wavy rectangular winglet pairs over the first tube. Near the inlet of heat exchanger surface the flow velocity is high. When the winglets are placed close to inlet, the pressure drop increases considerably resulting substantial rise in friction factor. When the first tube is not supported by either plain or wavy winglet, the

approaching velocity of the fluid to the winglet drops which is evident from Figs. 13(a-b). Due to this low velocity flow impingement at the front section of the adjacent tube the resulting pressure drop is relatively lower.

To summarize the overall effect of placement of the Plain and wavy rectangular winglet an enhancement factor is also presented in Table 2. The enhancement factor is found to be lower whenever the winglet pairs are located near the first or fourth tube. The former increases the pressure drop penalty whereas the later does not affect significant heat transfer enhancement. An optimum winglet location of P2W3 is found for both Re = 650 and 865. The heat transfer performance for this winglet position is maximum with moderate pressure drop penalty.

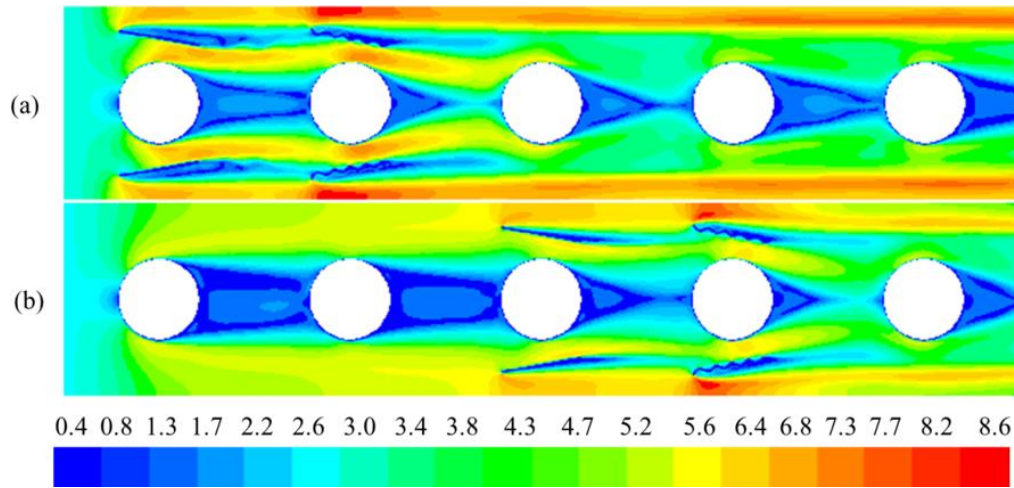


Fig. 13. Velocity contours (unit: m/s) over the fin surface for different combinations of Plain and wavy rectangular winglet: (a) P1W2, and (b) P3W4.

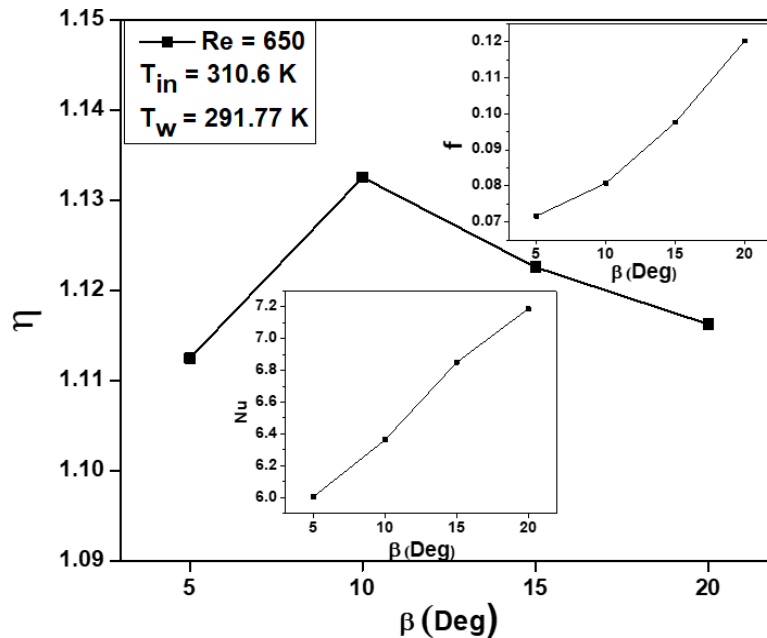


Fig. 14. Heat transfer and fluid flow parameters as a function of winglet's attack angle.

3.6 Effect of Wavy Winglet Attack Angle on Thermo-Fluid Performance

The effect of winglet attack angle on thermo-fluid performance has been investigated keeping the wave height and wave pitch constant. The attack angle is varied from 5°-20° with an interval of 5°. Figure 14 shows that the enhancement factor initially increases, attains maximum value at $\beta = 10^\circ$ and then drops. However, both Nu and f increases continuously with increase in β . With the increase in attack angle the thermally isolated wake region gets compressed and the flow impingement becomes more effective. This results in rich thermal mixing near the wake region. However, with advancement in β , the frontal area of the wavy winglet increases which in turn increases the form drag and results in considerably high pressure drop. As a result, the enhancement factor decreases

beyond $\beta = 10^\circ$.

4. CONCLUSIONS

The present CFD analysis was performed to assess the effect of wavy rectangular winglets on the heat transfer and fluid flow characteristics of a heat exchanger. The effect of variation in wavy winglet configuration has been examined numerically in detail. Some major findings are:

- I. It had been found out the friction factor was rising with wave number and the heat transfer was increased up to $n = 6$. An optimum wave number, $n = 6$ could be obtained where the enhancement factor was found to be maximum and for the present case it is 12-13% higher than baseline case.

- II. The heat transfer and friction factor were increased with increase in wave height. The enhancement factor was found to be maximum with an improvement of 13% over the baseline case corresponding to an optimum wave height of 0.9 mm.
- III. The impact of wavy winglet length on enhancement factor was found to be significant. An optimum enhancement factor could be obtained corresponding to 30 mm length where the enhancement factor is raised to 20% compared to baseline case.
- IV. Placement of combined wavy and plain winglets over the tubes plays an important role on heat transfer and fluid flow performance. When the plain winglet pair was placed over the second tube and wavy winglet pair over the third tube the enhancement factor was raised to a maximum of about 21% compared to baseline case.
- V. An attack angle of 10° was found to provide highest thermo-fluid performance with about 12-13% enhancement over baseline model.

The numerical analysis in the present study discusses the heat transfer and fluid flow performance of a fin-and-tube heat exchanger surface under laminar flow condition. The present work will be helpful in designing a compact and efficient heat exchanger for the air conditioning systems. Similar numerical investigations may be performed to obtain the optimum design value of different parameters under turbulent flow condition.

ACKNOWLEDGMENT

Authors are grateful to the Birla institute of technology, Mesra for providing Library facility and computational support to carry out the numerical analysis.

REFERENCES

- Arora, A., P. M. V. Subbarao and R. S. Agarwal (2015). Numerical optimization of location of “common flow up” delta winglets for inline aligned finned tube heat exchanger. *Applied Thermal Engineering* 82, 329-340.
- Caliskan, S. (2014). Experimental investigation of heat transfer in a channel with new winglet-type vortex generator. *International Journal of Heat and Mass Transfer* 78, 604-614.
- Chen, Y., M. Fiebig and N. K. Mitra (1998a). Conjugate heat transfer of a finned oval tube with a punched longitudinal vortex generator in form of a delta winglet- parametric investigations of the winglet. *International Journal of Heat and Mass Transfer* 41, 3961-3978.
- Chen, Y., M. Fiebig and N. K. Mitra (1998b). Heat transfer enhancement of a finned oval tube with punched longitudinal vortex generators in-line. *International Journal of Heat and Mass Transfer* 41, 4151-4166.
- Chimres, N., C. C. Wang and S. Wongwises (2018). Effect of elliptical winglet on the air-side performance of fin-and-tube heat exchanger, *International Journal of Heat and Mass Transfer* 123, 583-599.
- Chu, P., Y. L. He, Y. G. Lei, L. T. Tian and R. Li (2009). Three-dimensional numerical study on fin-and-oval-tube heat exchanger with longitudinal vortex generators. *Applied Thermal Engineering* 29(5-6), 859-876.
- Edwards, F. J. and C. J. R. Alker (1974, January). The improvement of forced convection surface heat transfer using surface protrusions in the form of (a) cubes and (b) vortex generators. *Proceedings of the 5th International Heat Transfer Conference*, Tokyo, Japan, 3, 244-248.
- Fiebig, M, P. Kallweit and N. K. Mitra (1986, January). Wing type vortex generators for heat transfer enhancement. *Proceedings of the 8th International Heat Transfer Conference San Francisco*, California, 6, 2909-2913.
- Fiebig, M., P. Kallweit, N. Mitra and S. Tiggelbeck (1991). Heat transfer enhancement and drag by longitudinal vortex generators in channel flow. *Experimental Thermal and Fluid Science* 4(1), 103-114.
- Gentry, M. C. and A. M. Jacobi (2002). Heat transfer enhancement by delta-wing-generated tip vortices in flat-plate and developing channel flows. *Journal of Heat Transfer* 124, 1158-1168.
- He, Y. L., P. Chu, W. Q. Tao, Y. W. Zhang and T. Xie (2013). Analysis of heat transfer and pressure drop for fin-and-tube heat exchangers with rectangular winglet-type vortex generators. *Applied Thermal Engineering* 61, 770-783.
- Jacobi, A. M. and R. K. Shah (1995). Heat transfer surface enhancement through the use of longitudinal vortices: A review of recent progress. *Experimental Thermal and Fluid Science* 11, 295-309.
- Joardar, A. and A. M. Jacobi (2007). A numerical study of flow and heat transfer enhancement using an array of delta-winglet vortex generators in a fin-and-tube heat exchanger. *Journal of Heat Transfer* 129(9), 1156-1167.
- Joardar, A. and A. M. Jacobi (2008). Heat transfer enhancement by winglet-type vortex generator arrays in compact plain-fin-and-tube heat exchangers. *International Journal of Refrigeration* 31(1), 87-97.
- Ke, H., T. A. Khan, W. Li, Y. Lin, Z. Ke, H. Zhu and Z. Zhang (2019). Thermal-hydraulic performance and optimization of attack angle of delta winglets in plain and wavy finned-tube heat exchangers. *Applied Thermal Engineering*

- 150, 1054-1065.
- Kobayashi, H., K. Yaji, S. Yamasaki and K. Fujita (2019). Freeform winglet design of fin-and-tube heat exchangers guided by topology optimization. *Applied Thermal Engineering* 161, 114020.
- Lemouedda, A., M. Breuer, E. Franz, T. Botsch, and A. Delgado (2010). Optimization of the angle of attack of delta-winglet vortex generators in a plate-fin-and-tube heat exchanger. *International Journal of Heat and Mass Transfer* 53, 5386-5399.
- Leu, J. S., Y. H. Wu and J. Y. Jang (2004). Heat transfer and fluid flow analysis in plate-fin and tube heat exchangers with a pair of block shape vortex generators. *International Journal of Heat and Mass Transfer* 47, 4237-4338.
- Li, M. J., W. J. Zhou, J. F. Zhang, J. F. Fan, Y. L. He and W. Q. Tao (2014). Heat transfer and pressure performance of a plain fin with radiantly arranged winglets around each tube in fin-and-tube heat transfer surface. *International Journal of Heat and Mass Transfer* 70, 734-744.
- Lu, G. and X. Zhai (2019). Effects of curved vortex generators on the air-side performance of fin-and-tube heat exchangers. *International Journal of Thermal Sciences* 136, 509-518.
- Naik, H. and S. Tiwari (2018). Effect of winglet location on performance of fin-tube heat exchangers with inline tube arrangement. *International Journal of Heat and Mass Transfer* 125, 248-261.
- Pesteei, S. M., P. M. V. Subbarao and R. S. Agarwal (2005). Experimental study of the effect of winglet location on heat transfer enhancement and pressure drop in fin-tube heat exchangers. *Applied Thermal Engineering* 25(11-12), 1684-1696.
- Russell, C. M. B., T. V. Jones and G. H. Lee (1982, January). Heat Transfer Enhancement Using vortex generators. *Proceedings of the 5th International Heat Transfer Conference* New York, 3, 283-288.
- Sarangi, S. K. and D. P. Mishra (2017). Effect of winglet location on heat transfer of a fin-and-tube heat exchanger. *Applied Thermal Engineering* 116, 528-540.
- Sarangi, S. K., D. P. Mishra and P. Mishra (2019). Analysis of Thermo-Fluid Performance of Fin-and-tube Heat Exchanger using Winglets. *ASME Journal of Heat Transfer*. (In Press).
- Sinha, A., H. Chattopadhyay, A. K. Iyengar and G. Biswas (2016). Enhancement of heat transfer in a fin-tube heat exchanger using rectangular winglet type vortex generators. *International Journal of Heat and Mass Transfer* 101, 667-681.
- Sohankar, A. and L. Davidson (2001). Effect of inclined vortex generators on heat transfer enhancement in a three-dimensional channel. *Numerical Heat Transfer Part A: Applications: An International Journal of Computation and Methodology* 39(5), 433-448.
- Tiggelbeck, S., N. K. Mitra and M. Fiebig (1994). Comparison of wing-type vortex generators for heat transfer enhancement in channel flows. *ASME Journal of Heat Transfer* 116(4), 880-885
- Wang, C. C. and Y. J. Chang (1996). Sensible heat and friction characteristics of plate fin-and-tube heat exchangers having Plain fins. *International Journal of Refrigeration* 19(4), 223-230.
- Wang, C. C., K. Y. Chen and Y. T. Lin (2015b). Investigation of the semi-dimple vortex generator applicable to fin-and-tube heat exchangers. *Applied Thermal Engineering* 88, 192-197.
- Wang, C. C., K. Y. Chen, J. S. Liaw and C. Y. Tseng (2015a). An experimental study of the air-side performance of fin-and-tube heat exchangers having plain, louver, and semi-dimple vortex generator configuration. *International Journal of Heat and Mass Transfer* 80, 281-287.
- Wang, Q., Z. Qian, J. Cheng, W. Huang and Jie Ren (2019). Analysis on thermal hydraulic performance of the elliptical tube in the finned-tube heat exchanger by new method. *International Journal of Heat and Mass Transfer* 134, 388-397.
- Wu, J. M. and W. Q. Tao (2011). Impact of delta winglet vortex generator on the performance of a novel fin-tube surfaces with two rows of tubes in different diameters. *Energy conversion and management* 52(8-9), 2895-2901.